

Electronic properties of Cs+CO coadsorbed on the Ru(0001) surface

Cite as: J. Chem. Phys. **108**, 774 (1998); <https://doi.org/10.1063/1.475437>

Submitted: 03 September 1997 . Accepted: 02 October 1997 . Published Online: 04 June 1998

S. Fichtner-Endruschat, V. De Renzi, A. Morgante, S. Schwegmann, H. Bludau, R. Schuster, A. Böttcher, and H. Over



View Online



Export Citation

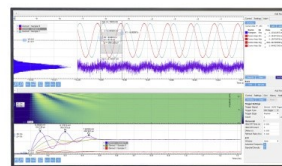
ARTICLES YOU MAY BE INTERESTED IN

[Anomalous hydrogen adsorption sites found for the \$c\(2\times 2\)-3H\$ phases formed on the Re\(10 \$\bar{1}\$ 0\) and Ru\(10 \$\bar{1}\$ 0\) surfaces](#)

The Journal of Chemical Physics **108**, 8671 (1998); <https://doi.org/10.1063/1.476296>

Challenge us.

What are your needs for
periodic signal detection?



Zurich
Instruments



Electronic properties of Cs+CO coadsorbed on the Ru(0001) surface

S. Fichtner-Endruschat and V. De Renzi

Fritz-Haber-Institut der Max-Planck-Gesellschaft, Faradayweg 4-6, D-14195 Berlin, Germany

A. Morgante

T.A.S.C.-I.N.F.M. Laboratory, Padriciano 99, I-34012 Trieste, Italy

S. Schwegmann, H. Bludau, and R. Schuster

Fritz-Haber-Institut der Max-Planck-Gesellschaft, Faradayweg 4-6, D-14195 Berlin, Germany

A. Böttcher

Humboldt-Universität zu Berlin, Institut für Physik, Oberflächenphysik und Atomstoßprozesse, Invalidenstrasse 110, D-10115 Berlin, Germany

H. Over^{a)}

Fritz-Haber-Institut der Max-Planck-Gesellschaft, Faradayweg 4-6, D-14195 Berlin, Germany

(Received 3 September 1997; accepted 2 October 1997)

The variation of the Cs 6*s* and the Cs 5*p* emission in He* and Ne* metastable deexcitation spectroscopy (MDS) as a function of the CO exposure indicates a demetallization of the Ru(0001)–(2×2)-Cs and the Ru(0001)–($\sqrt{3}\times\sqrt{3}$)R30°-Cs surfaces upon CO coadsorption. This observation corroborates a (substrate-mediated) charge transfer from the Cs atom to the 2*π** orbital of CO. With the Ru(0001)–(2×2)-Cs system even at CO saturation, MD spectra show emission associated with the Cs 6*s* state, indicating that the Cs atoms are not completely ionized. Exposing the ($\sqrt{3}\times\sqrt{3}$)R30°-Cs-pre-covered Ru(0001) to CO, surplus Cs of the first layer is displaced into a second layer. In this way, CO molecules are able to be accommodated into the first layer. Desorbing this second layer Cs by heating the sample to 600 K produces a (2×2) structure with one Cs and CO in the unit cell as evidenced by MDS and low energy electron diffraction. © 1998 American Institute of Physics. [S0021-9606(98)02902-X]

I. INTRODUCTION

The coadsorption of CO and alkali metals on transition metal surfaces has been envisioned as a workhorse to study the role of alkali metals as promoters in catalytic reactions, such as carbon monoxide hydrogenation and oxidation.¹ Most of the work has been performed for K and CO coadsorbed on various metal surfaces concentrating on their electronic and vibrational properties.^{1,2} These studies were, however, based on *ad hoc* assumptions about the atomic geometry of this coadsorption system since this piece of information was not available at that time.³

Recently, the coadsorption of CO and Cs on Ru(0001) has been investigated,^{4,5} thereby providing detailed information on the atomic geometry and the vibrational properties. However, for this particular system the electronic properties are hardly known. Starting from a (2×2)-Cs-pre-covered Ru(0001) surface, coadsorption of CO leads to an improved ordering and the formation of the mixed Cs+CO overlayer. A corresponding low energy electron diffraction (LEED) structure analysis⁶ indicated that Cs atoms remain in on-top position (as also found for Ru(0001)–(2×2)-Cs⁷), while the CO molecule changes its adsorption site from on top, as found on the clean Ru(0001) surface,⁸ to the threefold hollow site in the mixed Cs+CO overlayer. This site change was ascribed to a purely electronic effect. CO molecules can

utilize the enhanced charge density at the surface due to the Cs overlayer by a (substrate-mediated) charge transfer into the 2*π** CO molecular orbital. Since back donation is more efficient in highly coordinated sites than in on-top positions, CO changes its adsorption site. This view of modified CO–Ru bonding is corroborated by a recent high resolution electron energy loss spectroscopy (HREELS) study which indicated a lowering of the C–O stretch vibrational frequency upon Cs coadsorption.⁴ In addition, this HREELS study indicated that the original “metallization” of the Cs(2×2) overlayer, i.e., the delocalization of the Cs 6*s* electron wave function across the surface, is removed by coadsorbed CO molecules.

Starting instead with a full monolayer of Cs, i.e. a ($\sqrt{3}\times\sqrt{3}$)R30°-Cs structure, CO uptake is slowed down by at least two orders of magnitude. Still, some CO can stick to the surface, eventually forming a bond with the Ru substrate and simultaneously forcing some of the Cs atoms to move from the first to the second layer.⁹ Altogether these findings demonstrate an intimate interrelation of geometric and vibrational properties with electronic properties which motivated us to study the Cs+CO coadsorption system on Ru(0001) with spectroscopic methods such as metastable deexcitation spectroscopy (MDS) and ultraviolet photoelectron spectroscopy (UPS). The combination of UPS and MDS is particularly useful since it allows to discriminate between electronic properties merely of the outermost layer (MDS) and those of a slab consisting of several layers (UPS). Additionally, MDS is quite sensitive to *s*-like charge density, while UPS is not.

^{a)} Author to whom correspondence should be addressed. Electronic mail: over@fhi-berlin.mpg.de; Fax: ++49-30-84135106.

On transition metal surfaces MDS allows the investigation of states close to the Fermi level which are created by the formation of the chemisorption bond. These states are usually masked in UPS by strong emission from the metallic *d* states so that both techniques are complementary to some extent. Recent MDS measurements of Li and Na films on Ru(0001) have shown that the state of metallization^{10,11} can be readily monitored by MDS.

II. EXPERIMENTAL DETAILS

The measurements were conducted on the same Ru(0001) sample in different ultrahigh vacuum (UHV) chambers. One chamber⁵ contains a four-grid back-view LEED optics, auger electron spectroscopy (AES), thermal desorption spectroscopy (TDS), and facilities to clean and prepare the Ru(0001) surface. The sample temperature can be varied from 40 K (by cooling with liquid He) to 1530 K (by direct resistive heating). The other experimental system¹² consists of an atomic beam source in which metastable noble gas atoms (either He or Ne) are produced by electron impact. The atomic beam source is connected with the spectrometer chamber equipped with standard facilities for sample preparation, a He discharge lamp for UPS, and a hemispherical electron energy analyzer for recording the kinetic energy distribution of electrons emitted from the surface. The metastable atoms are deexcited upon colliding with the sample surface which causes the emission of electrons from the outermost layer of the surface. For the kinetic energy of the emitted electrons an energy balance analogous to UPS holds. The use of He or Ne metastable atoms allows to preferentially probe orbitals either with σ symmetry or with π symmetry, respectively.^{13(b)} Since the work function of the sample surface was below 3 eV in all of our measurements, the major deexcitation mechanism of the metastable noble gas atoms is Penning ionization, i.e., an electron transition from states of the mixed Cs+CO overlayer into the ground state hole of the impinging metastable atom is accompanied by the emission of the electron from the metastable state orbital.^{13(a)} This electron carries the energy difference between the excitation energy of the He* and the binding energy of the electron from the surface and, hence, directly probes the density of states of the outermost surface layer.

Cesium was evaporated from well outgassed dispenser sources (SAES Getter, Inc.). At a sample temperature of 220 K the deposition rate was about 1 ML/min. Specific submonolayer coverages were prepared by first evaporating an alkali metal layer of approximately 2 ML, followed by flash annealing to predetermined temperatures to desorb excess alkali metal. The $(\sqrt{3} \times \sqrt{3})R30^\circ$ -Cs and the (2×2) -Cs overlayers need annealing to temperatures of 332 and 523 K, respectively (heating rate 5 K/s). CO (99.97%) was dosed by backfilling the chamber with a partial pressure of 1×10^{-8} mbar.

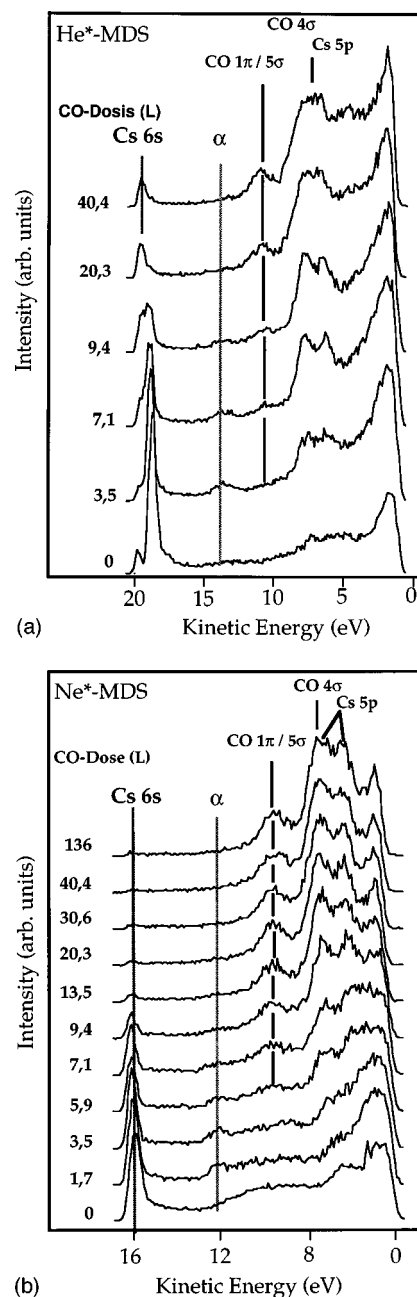


FIG. 1. (a) He* MD spectra and (b) Ne* MD spectra from a (2×2) -Cs-precovered Ru(0001) surface which is exposed to various amounts of CO as specified in the figure.

III. RESULTS AND DISCUSSION

A. CO adsorption on the (2×2) -Cs-precovered Ru(001) surface

Figure 1 shows He* MD spectra from a (2×2) -Cs-precovered Ru(0001) surface which is exposed to increasing amounts of CO. The electron emission is shown as a function of the kinetic energy. A representation in terms of binding energies would require the knowledge of the effective excitation energy of the impinging metastable He or Ne atoms which is in general influenced by the chemical composition of the outermost surface. For metal surfaces this leads to variations of E^* of several 100 meV.¹³ As discussed in detail

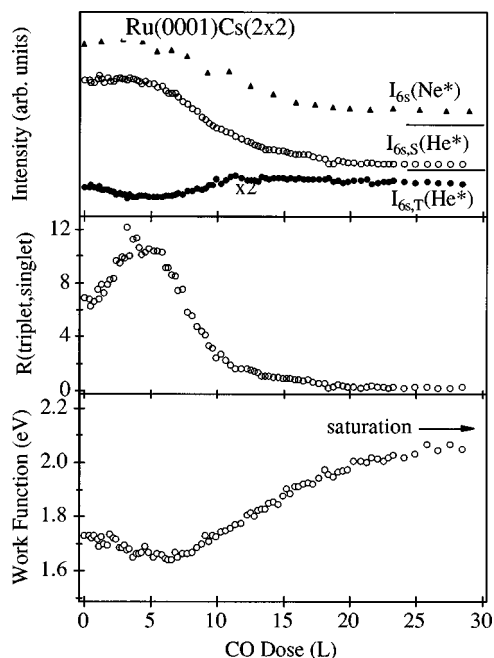


FIG. 2. The intensity of the Cs $6s$ -derived peaks in He* and Ne* MDS, singlet–triplet conversion rate R , and the work function change during CO exposure of the (2×2) -Cs-pre-covered Ru(0001) surface.

in Ref. 10 the emission of electrons with highest kinetic energy originates from the Cs $6s$ level excited by either singlet (20.3 eV) or triplet (19.1 eV) He* atoms. Since the majority ($\geq 90\%$) of impinging metastable He* atoms are originally in the singlet state [He*(2^1S)], and the MD spectra show a strong Cs $6s$ emission at a kinetic energy related to the He triplet state, an efficient singlet–triplet conversion has taken place prior to the actual deexcitation process reflecting the presence of a rather metallic Cs overlayer.¹¹ As summarized in Fig. 2, with progressing CO exposure, the total emission from the Cs $6s$ level decreases monotonically, whereas the singlet–triplet conversion rate R (defined as the ratio of singlet to triplet peak intensity in MDS) increases first before it decreases steeply beyond 9 L. The maximum of R is related to the minimum of the work function change $\Delta\Phi$; the work function change was determined by the width of the UPS spectra. The decrease of R is consistent with a gradual “demetallization”¹⁰ of the surface due to CO adsorption as also observed with HREELS.⁴ Regardless of the specific mechanisms suggested in the literature,^{11,14} the singlet–triplet conversion step prior to the final Penning ionization step requires both occupied and unoccupied states near the Fermi level, i.e., a metallic surface. It is remarkable that, even for high CO exposures, a $6s$ -derived MD signal is discernible which implies that the Cs atoms are still not completely ionized.

Electron emission with smaller kinetic energy (He*MDS) is assigned to $5\sigma+1\pi$ of CO (≈ 10 eV) and to the Cs $5p$ -derived states (≈ 8 eV). The assignment was made by comparison with the corresponding UP spectrum for which energy levels are known from the literature.^{15,16} As expected, the intensity of the $5\sigma+1\pi$ -derived peak at about 10 eV

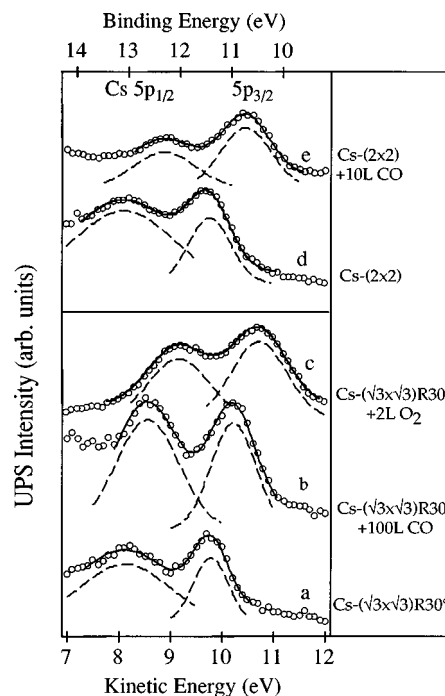


FIG. 3. UP spectra in the energy region of the Cs $5p$ doublet for various overlayers on Ru(0001): (a) $(\sqrt{3} \times \sqrt{3})R30^\circ$ -Cs clean, (b) $(\sqrt{3} \times \sqrt{3})R30^\circ$ -Cs+100 L CO, (c) $(\sqrt{3} \times \sqrt{3})R30^\circ$ -Cs+2 L O₂, (d) (2×2) -Cs clean, (e) (2×2) -Cs+10 L CO.

increases gradually with CO exposure [cf. Fig. 1(a)]. The electron emission from the 4σ CO state overlaps with the signal originating from the Cs $5p$ states and is therefore obscured.

The Cs $5p$ doublet shifts to lower binding energies upon CO adsorption as evidenced by UPS (Fig. 3(d) and 3(e)); a similar effect was also observed for oxygen adsorption on a Cs-pre-covered Ru(0001) surface.¹⁷ Intuitively one would expect to find a shift of the Cs $5p$ levels to larger binding energies since the transfer of Cs $6s$ charge density to the CO molecules should lead to a reduction of the screening charge density in the core region, thus increasing the binding energies of the Cs $5p$ core levels. On the other hand, it is frequently observed that a core level shifts to lower binding energy when the coordination of the respective species is increased, i.e., when the adsorbate atoms are less exposed to the vacuum.¹⁸

The negative chemical shift of the Cs $5p$ levels can alternatively be explained by a charge redistribution between $6s$ and $5d$ levels of Cs, as first proposed for BaO¹⁹ and later modified for the case of Cs oxides.²⁰ According to this model, Cs loses $6s$ charge density but concomitantly receives $5d$ charge density. This effect is a consequence of the surface compression of the Cs overlayer due to the bond formation of Cs with the topmost Ru layer; recall that a $6s \rightarrow 5d$ charge transfer is also found for Cs bulk material which is subject to high external pressures.²¹ As a net result, the Cs $6s$ becomes more strongly polarized towards the Ru(0001) substrate. The population of $5d$ states, however, causes the Cs $5p$ levels in UPS and MDS to shift to lower binding energies. Coadsorbing CO molecules squeeze into

the Cs overlayer which compresses the Cs charge density in the (2×2)-Cs overlayer, thus enforcing the $6s5d$ hybridization. This might result in the observed shift of the Cs $5p$ levels in UPS and MDS. In other words, coadsorbing CO molecules even further polarize the Cs $6s$ state toward the Ru substrate. The stronger Cs $6s$ polarization toward Ru is also supported by the evolution of the Cs $5p$ emission in He* MDS [cf. Fig. 1(a)] which increases markedly with CO exposure. Obviously, the coadsorbed CO molecules consume the (delocalized) Cs $6s$ charge density in the overlayer which in turn leads to an improved exposure of Cs $5p$ orbitals to the impinging metastable He* and Ne* atoms.

Similar to the case of K+CO on Ru(0001),¹⁵ but different from the case of K+CO on Ni(111),²² no $2\pi^*$ -derived molecular orbital was seen in the MD spectra for the Cs-pre-covered Ru(0001) surface. The MD spectra (Fig. 1) do reveal intense electron emission from the $5\sigma+1\pi$ of CO. Recalling the particular shapes of the 5σ and 1π molecular orbitals,²³ the 1π orbital reaches farther out into the vacuum region than the 5σ orbital. Hence, it is plausible to assume that the CO ($5\sigma+1\pi$) emission consists mainly of electrons ejected from the 1π orbital, as also concluded by Jänsch *et al.*²⁴ The Ne* MD spectra of the same system [shown in Fig. 1(b)] are quite similar to those spectra taken with He* atoms [cf. Fig. 1(a)]. The main difference is the improved resolution of the Cs $5p$ levels in the Ne MD spectrum since Ne* is expected to be more sensitive to orbitals with π symmetry than He*. An additional feature, which becomes more obvious in Ne* MD spectra than in corresponding He* MD spectra, is the narrowing of the Cs $5p_{1/2}$ linewidth upon coadsorption of CO, the Cs $5p_{3/2}$ linewidth remains constant.

In Fig. 4 we compare the spectra of He* and Ne* MDS with corresponding UPS measurements. There is a one-to-one correspondence of peaks in the Ne* MD spectrum with those in the UP spectrum but in the He* MD spectrum the Cs $5p$ and CO ($5\sigma+1\pi$) associated peaks are shifted by 0.8 eV to higher binding energies. As this shift is similar to the energy difference between singlet and triplet metastable He atoms, one might interpret the Cs $5p$ and CO ($5\sigma+1\pi$) emissions in the He MD spectra as due to quenching of triplet He atoms.

Next, we concentrate on the region between 10 and 5 eV kinetic energy in MD and UP spectra where a CO-alkali metal hybrid state is discussed for CO/K/Ru(0001)¹⁵ and called “ α ” peak (cf. Fig. 1). A feature at 12 eV emerges in Ne* MDS (and at 14 eV in He* MDS) with ongoing CO deposition and disappears finally beyond 10 L. This CO-derived peak (α) is not present in the pure CO spectrum, and therefore it might be attributed to the intense Cs–CO interaction. It was carefully checked that neither oxygen impurity in the CO gas and CO dissociation nor background gas adsorption during the experiment were responsible for these emissions. MDS is sensitive to orbitals which are polarized toward the vacuum region and to orbitals with σ symmetry. Therefore, considering the high intensity in MDS, the α state is interpreted to be polarized toward the vacuum. A comparison of the evolution of α with those of the singlet–triplet conversion rate R and the intensity of Cs $6s$ reveals a close

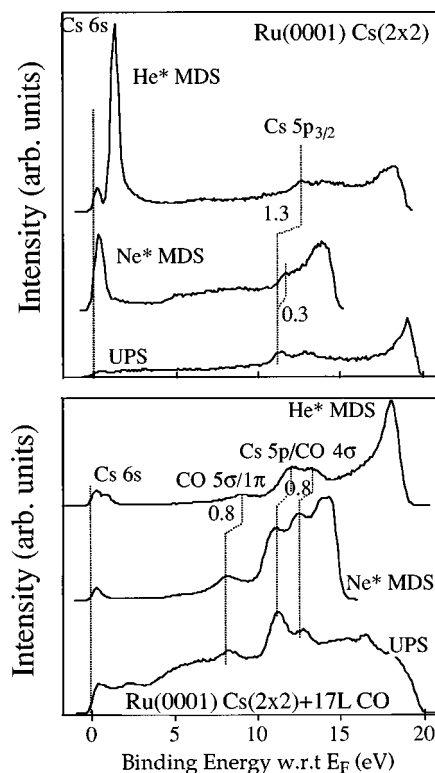


FIG. 4. Comparison of He* and Ne* MD spectra with corresponding UP spectra for (a) Ru(0001)-(2×2)-Cs and (b) Ru(0001)-(2×2)-Cs+17 L CO.

relation between α and the demetallization of the surface. The interaction of CO with this delocalized Cs $6s$ charge density leads to the electron emission α . With prolonged CO exposure the delocalized Cs $6s$ density diminishes with the consequence that α also disappears in MDS. Hence, one might argue that the α peak represents a direct interaction of delocalized Cs $6s$ charge density with the CO molecule.

In Fig. 3 we compare the Cs $5p$ -associated features in UPS of the Cs-pre-covered Ru(0001) surfaces with those of the Cs+CO and Cs+O-covered Ru(0001) surfaces. The most remarkable variation in these spectra is the linewidth of the Cs $5p_{1/2}$ level. Upon CO exposure, the Cs $5p_{1/2}$ profile narrows quite substantially. Without CO, the emission from the Cs $5p_{1/2}$ level is quite broad since the core hole is filled rapidly by an electron from the Cs $5p_{3/2}$ which leads to electron emission from the Cs $6s$ band via an Auger-like transition. The direct Cs $5p_{1/2}$ -Cs $5p_{3/2}$ transition is dipole forbidden. Therefore, the presence of Cs $6s$ charge density close to the Fermi level is mandatory for this so-called Coster–Kronig transition to be efficient. The emitted electrons have very low kinetic energy and are usually obscured by the secondary electron emission in UPS. If we now add CO and O (both are electronegative species) to the Cs overlayer, the Cs $6s$ charge density is gradually depleted through a charge transfer from Cs to CO or O. This process reduces the probability for a Coster–Kronig transition and therefore increases the lifetime of the Cs $5p_{1/2}$ hole which in turn narrows the Cs $5p_{1/2}$ profile as evidenced in UPS.

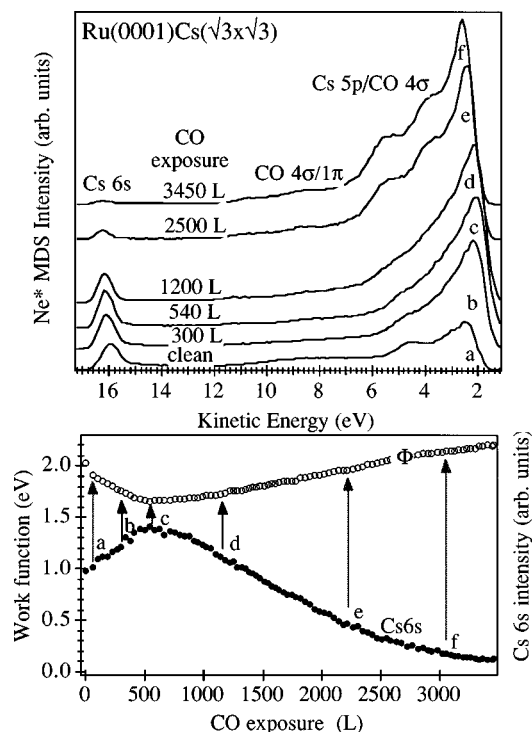


FIG. 5. (a) Ne* MD spectra from a $(\sqrt{3} \times \sqrt{3})R30^\circ$ -Cs-pre-covered Ru(0001) surface which is exposed to increasing amounts of CO as specified in the figure. (b) The intensity of the Cs 6s emission in comparison with the work function change.

B. CO adsorption on the $(\sqrt{3} \times \sqrt{3})R30^\circ$ -Cs-pre-covered Ru(0001) surface

The Ne MD spectra of Ru(0001)- $(\sqrt{3} \times \sqrt{3})R30^\circ$ -Cs exposed to increasing doses of CO are summarized in Fig. 5. The Cs 6s-derived MD signal $I(6s)$ first increases until the work function has passed the minimum and then decreases at higher doses [Fig. 6(b)]; note that the singlet-triplet splitting is too small to be resolved for metastable Ne atoms. The behavior of the 6s emission is in contrast to that observed for the (2×2) -Cs-pre-covered surface for which this emission in the Ne* MD spectra steadily decreases with CO exposure. Additionally, on the $(\sqrt{3} \times \sqrt{3})R30^\circ$ -Cs surface the sticking coefficient is two orders of magnitude smaller than for the (2×2) -Cs. Hence, the demetallization of the $(\sqrt{3} \times \sqrt{3})R30^\circ$ -Cs surface needs much higher CO doses [cf. Fig. 5(b)].

He MD spectra from the $(\sqrt{3} \times \sqrt{3})R30^\circ$ -Cs-pre-covered Ru(0001) surface exposed to 200 L CO (cf. Fig. 6) reveal a surprisingly high Cs 6s-derived signal. Concomitant LEED measurements of this surface show a complex LEED pattern with dominating spots at positions of a rotated (2×2) structure. A similar LEED pattern was also reported by Kondoh and Nozoye.⁹ Upon heating this overlayer to 600 K, the MD spectrum transforms into a spectrum which is identical to that from the (2×2) -Cs+CO surface prepared at room temperature. From TDS measurements, on the other hand, it is found that part of the Cs desorbs during this annealing process (while all CO molecules stay on the surface), leaving a well-ordered (2×2) structure behind as indicated by the

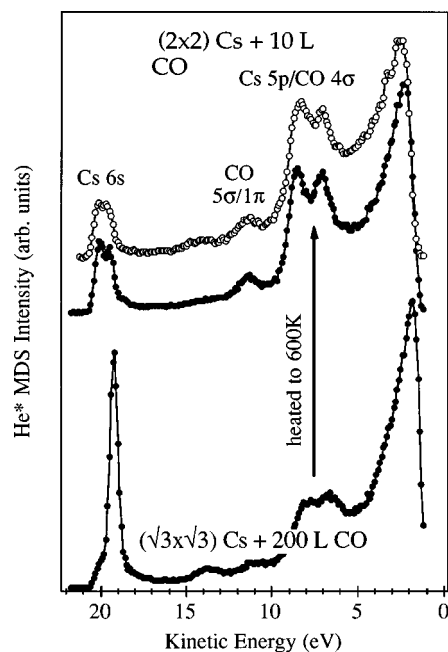


FIG. 6. He* MD spectra from the $(\sqrt{3} \times \sqrt{3})R30^\circ$ -Cs-pre-covered Ru(0001) surface exposed to 200 L CO and after annealing to 600 K in comparison with the He* MD spectrum of the Ru(0001)- (2×2) -Cs+10 L CO.

LEED pattern. LEED $I-V$ curves taken for this *a priori* unknown (2×2) structure are almost identical to those found for the (2×2) -Cs+1CO phase but significantly different from LEED $I-V$ curves of the (2×2) -Cs+2CO phase.⁵ Therefore, this (2×2) phase can safely be ascribed to a (2×2) -Cs+1CO overlayer. The question left is where the excess Cs was located prior to desorption via heating to 600 K: Either the Cs atoms were placed on top of the mixed (2×2) -Cs+1CO layer, or they could have been embedded in the Cs+1CO layer. The strong Cs 6s emission in MDS after CO exposure, however, evidences the formation of a second Cs layer on top of the Cs+1CO layer.

The finding of second layer Cs is also consistent with the experimentally observed variation of the emission of Cs 5p and the $5\sigma+1\pi$ -CO which are both significantly larger after than before heating the sample to 600 K. With Cs in the second layer, these features are substantially damped, while after removing the second layer Cs atoms, the Cs 5p and also the CO-($5\sigma+1\pi$)-derived emissions are appreciably enhanced. Altogether these findings confirm the formation of second layer Cs atoms upon adsorption of CO onto the $(\sqrt{3} \times \sqrt{3})R30^\circ$ -Cs surface, as has already been proposed by Kondoh and Nozoye.⁹

The above picture is comprehensive only for CO doses up to 1000 L. When exposing the $(\sqrt{3} \times \sqrt{3})R30^\circ$ -Cs surface to even higher CO doses (3500 L), some drastic changes occurred in thermal desorption spectra (cf. Fig. 7). The thermal desorption of CO, Cs, and CO_2 was monitored simultaneously. While for the case of 1000 L CO. [cf. Fig. 7(a)], only very few CO_2 could be detected; the CO_2 signal increases by a factor of 8 when dosing 3500 L CO instead [cf. Fig. 7(b)]. Since the CO exposure is increased only by a

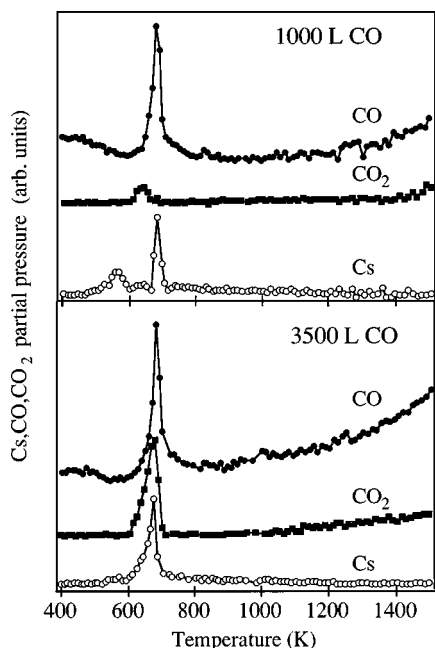


FIG. 7. Thermal desorption spectra of Cs, CO, and CO₂. The Ru(0001)-($\sqrt{3} \times \sqrt{3}$)R30°-Cs surface is exposed to (a) 1000 L CO (b) 3500 L CO.

factor of 3.5 at fixed CO partial pressure, this effect cannot be simply related to CO₂ stemming from the residual gas or from the impurity concentration of the admitted CO gas. Parallel with this increase in CO₂ production, the Cs TD spectrum also changed. The weaker bound Cs, which is attributed to second layer Cs, disappears for the case of 3500 L CO, and instead the co-desorption peak broadens and shifts to lower temperatures. The LEED patterns are also quite different. While for the 1000 L CO case the above mentioned complex rotated (2×2) LEED pattern is observed, the LEED pattern for the 3500 L CO case exhibits only simple (2×2) symmetry. Accompanying MDS measurements still show small emission due to the Cs 6s for 1000 L CO, but this signal is largely suppressed upon CO exposure of 3500 L. One may speculate that excessive CO exposure also turns the second layer Cs atoms into a more or less ionized species, which is involved in the production of CO₂, or second layer Cs atoms simply desorb.

IV. CONCLUSIONS

The variation of the electron emission in MDS due to the Cs 6s level as a function of the CO exposure indicates a demetallization of the Cs(2×2) and the ($\sqrt{3} \times \sqrt{3}$)R30°-Cs overlayer upon CO coadsorption. This observation is in line with the interpretation of recent HREELS measurements⁴ and corroborates the idea of a pronounced (substrate-mediated) charge transfer from the Cs atom to the $2\pi^*$ orbital of CO. Even at CO saturation, the Cs atoms are not completely ionized in the (2×2)-Cs overlayer, as MD spectra still show an emission associated with Cs 6s level. The Cs-CO interaction manifests itself in the presence of a Cs-CO hybrid orbital (α) in MDS, which is polarized to-

ward the vacuum and disappears beyond a CO exposure of 10 L. One might argue that the α peak is related to a direct interaction of delocalized Cs 6s charge density with CO. Beyond a CO exposure of 10 L this interaction is suppressed due to demetallization.

The high-density ($\sqrt{3} \times \sqrt{3}$)R30°-Cs-pre-covered Ru(0001) surface reveals some additional features. Upon adsorption of CO, part of the Cs in the first layer is displaced into a second layer which enables the CO molecules to accommodate into the first layer. Removing this second layer Cs by heating the sample to 600 K produces a surface which is identical to the (2×2)-Cs+1CO phase as evidenced by MDS and LEED. However, if the ($\sqrt{3} \times \sqrt{3}$)R30°-Cs surface is exposed to even higher doses of CO (e.g., 3500 L), the Cs 6s signal in MDS diminishes, and simultaneously a species is created that leaves the surface as CO₂, as evidenced by TDS measurements.

ACKNOWLEDGMENTS

We appreciate very much the valuable discussions with J. N. Andersen, K. Jacobi, and G. Ertl. V.D. acknowledges partial financial support from A. Della Riccia Foundation.

- ¹G. Pirug and H. P. Bonzel, in *The Chemical Physics of Solid Surfaces, Coadsorption, Promoters, and Poisons*, edited by D. A. King and D. P. Woodruff (Elsevier, Amsterdam, 1993), Vol. 6, pp. 51–112.
- ²*Physics and Chemistry of Alkali Adsorption*, edited by H. P. Bonzel, A. M. Bradshaw, and G. Ertl (Elsevier, Amsterdam, 1989).
- ³R. D. Diehl and R. McGrath, *Surf. Sci. Rep.* **23**, 43 (1996).
- ⁴K. Jacobi, H. Shi, M. Gruyters, and G. Ertl, *Phys. Rev. B* **49**, 5733 (1994).
- ⁵H. Over, H. Bludau, R. Kose, and G. Ertl, *Surf. Sci.* **331–333**, 62 (1995).
- ⁶H. Over, H. Bludau, R. Kose, and G. Ertl, *Phys. Rev. B* **51**, 4661 (1995).
- ⁷H. Over, H. Bludau, M. Skottke-Klein, G. Ertl, W. Moritz, and C. T. Campbell, *Phys. Rev. B* **45**, 8638 (1992).
- ⁸G. Michalk, W. Moritz, H. Pfnür, and D. Menzel, *Surf. Sci.* **129**, 92 (1983).
- ⁹H. Kondoh and H. Nozoye, *Surf. Sci.* **334**, 39 (1995).
- ¹⁰A. Böttcher, A. Morgante, R. Grobecker, T. Greber, and G. Ertl, *Phys. Rev. B* **49**, 10607 (1994).
- ¹¹B. Woratschek, W. Sesselmann, J. Küppers, G. Ertl, and H. Haberland, *Phys. Rev. Lett.* **55**, 611 (1985).
- ¹²H. Conrad, G. Ertl, J. Küppers, W. Sesselmann, and H. Haberland, *Surf. Sci.* **121**, 161 (1982).
- ¹³(a) W. Sesselmann, B. Woratschek, G. Ertl, J. Küppers, and H. Haberland, *Surf. Sci.* **146**, 14 (1984); (b) G. Ertl and J. Küppers, *Low Energy Electron and Surface Chemistry* (VCH, Weinheim, 1985).
- ¹⁴R. Hemmen and H. Conrad, *Phys. Rev. Lett.* **67**, 1314 (1991).
- ¹⁵G. H. Rucker, C. Huang, C. L. Cobb, H. Metiu, and R. M. Martin, *Surf. Sci.* **244**, 103 (1991).
- ¹⁶T. K. Sham and J. Hrebek, *J. Chem. Phys.* **89**, 1188 (1988).
- ¹⁷G. Ebbinghaus, W. Braun, A. Simon, and K. Berresheim, *Phys. Rev. Lett.* **37**, 1779 (1976).
- ¹⁸W. F. Egelhoff, Jr., *Surf. Sci. Rep.* **6**, 253 (1987); A. Nilsson, B. Eriksson, N. Mårtensson, J. N. Andersen, and J. Onsgard, *Phys. Rev. B* **38**, 10357 (1988).
- ¹⁹G. K. Wertheim, *J. Electron Spectrosc. Relat. Phenom.* **34**, 309 (1984).
- ²⁰J. A. Rodriguez, J. Hrebek, M. Kuhn, and T. K. Sham, *J. Phys. Chem.* **97**, 4737 (1993).
- ²¹M. Ross and A. K. McMahan, *Phys. Rev. B* **26**, 4088 (1982).
- ²²J. Lee, C. P. Hanrahan, J. Arias, R. M. Martin, and H. Metiu, *Phys. Rev. Lett.* **51**, 1803 (1983).
- ²³J. C. Campuzano, in *Chemical Physics of Solid Surfaces and Heterogeneous Catalysis*, edited by D. A. King and D. P. Woodruff (North-Holland, Amsterdam, 1990), Vol. 3(a).
- ²⁴H. J. Jänsch, C. Huang, A. Ludviksson, J. D. Redding, H. Metiu, and R. M. Martin, *Surf. Sci.* **222**, 199 (1989).